Mathematical Physics, chapter 17. Cambridge: Univ. Press.

KATO, N. (1952). *J. Phys. Soc. Jap.* **7**, 397.

KATO, N. (1955). *J. Phys. Soc. Jap.* **10**, 46.

KATO, N. (1958). *Acta Cryst.* **11**, 885.

KATO, N. (1960). *Acta Cryst.* **13**, 349.

KATO, N. & LANG, A. R. (1959). *Acta Cryst.* **12**, 787.

LAUE, M. V. (1952). *Acta Cryst.* **5**, 619.

SNEDDON, I. N. (1951). *Fourier Transforms*, Table II. New York: McGraw-Hill.

WALLER, I. (1926). *Ann. Phys.* **79**, 261.

WATSON, G. N. (1944). *A Treatise on the Theory of Bessel Functions*, p. 32. Cambridge: Univ. Press.

ZACHARIASEN, W. H. (1945). *Theory of X-ray Diffraction in Crystals*, Section III, p. 8. New York: Wiley.

Orientated Crystal Growth in Electrodeposits, in Relation to Ionic Diffusion in the Electrolyte

By H. I. MATTHEWS, T. DE S. MUTUCUMARANA AND H. WILMAN

Applied Physical Chemistry of Surfaces Laboratory, Chemical Engineering Department, Imperial College, London, S.W. 7, England

The structure and form of dendritic Cu and Ag electrodeposits from $CuSo_4$ and $AgNO_3$ solution are studied as a function of the current density (i) and time of deposition (t), by means of light microscopy, electron microscopy and electron diffraction. The structure and orientation are considered particularly in relation to the time τ of deposition giving first visible dimming of an initially smooth cathode ($i\sqrt{\tau} = $ constant), and also in relation to the observed crystal habit. The micrographs show that the crystals have pronounced {111} faces parallel to the plane of the stems and branches of the dendrites. This is associated with a preferred orientation of the deposit with a $\langle 110 \rangle$ direction normal to the cathode, although in several cases $\langle 210 \rangle$ orientation was developed. The details of the electron micrographs indicate that the dendrites arise from the pronounced preferential deposition of cations on projecting parts of the cathode owing to their motion being limited by diffusion. This diffusion effect also accounts for the variation, with current density, of the deposit thickness at which twinning develops, in the results of Setty & Wilman (1955).

1. Introduction

Electron-diffraction experiments in this laboratory (Finch & Sun, 1936; Finch & Williams, 1937) showed that metal electrodeposits at low current densities tend to grow as crystals having the most densely populated atomic plane parallel to the substrate ('lateral growth'). Those formed at higher current densities tend to develop a preferred crystal orientation with the most densely populated lattice row normal to the substrate ('outward growth').

Finch, Wilman & Yang (1947) have shown that, even in the 'lateral' type of growth on a smooth electropolished substrate, preferential deposition on small projections of the cathode surface occurs and leads to progressive roughening of the deposit surface. Furthermore, it was concluded that 'outward growth', with its characteristic preferred orientation, was due to this tendency, and was favoured by low bath temperature, low concentration of the electrolyte, high current density, and absence of stirring. All these features indicate that such growth is due to the rapid impoverishment of the solution near the cathode, with respect to the cations, and the slowness of their replacement by diffusion from regions of solution

further away from the cathode. Under conditions very strongly favouring outward growth, the deposits develop as needle-shaped or dendritic crystals having the above characteristic orientation (Finch & Layton, 1951).

In view of the present importance of such deposits for preparation of powders suitable for use in powder metallurgy, we have now examined this 'outward' type of cathodic crystal growth in more detail in the case of copper and silver. The results, described below, are considered in relation to the published results on the change in cation concentration near the cathode as deposition proceeds, and the related stage of visual dimming or roughening of the cathode, which is observed after a time τ of deposition given by $i\sqrt{\tau} = $ constant (Ullman, 1897; Sand, 1900, 1901; Sebborn, 1933; Kudra, 1934, 1935, 1936, 1937, 1938a, b; Kaneko & Kawamura, 1940; Wranglen, 1950; Ibl & Trümpler, 1952, 1953; Modi & Tendolkar, 1953; Ibl 1954).

2. Experimental

Electrodeposits were prepared from 0·1 and 0·3M $CuSO_4$ and 0·1M $AgNO_3$ solutions in water, about

300 cm.[3] being used at a time in a pyrex beaker, without stirring, at room temperature, and with a nominal current density in the range 1–100 mA. cm.$^{-2}$. Copper and silver anodes respectively were used. Substrates consisted of copper, silver and stainless-steel discs, about 1 cm. in diameter, smoothed on emery papers down to 0000 grade and polished with 'Bluebell' metal polish. The deposits were rinsed in distilled water, then in acetone to remove the water (which tends to cause formation of Cu_2O on the copper), and at once transferred to the electron-diffraction camera (Finch & Wilman, 1937) and evacuated by the rotary oil pump and oil-vapour diffusion pumps. Approximately 60 kV. electrons were used, with a camera length of about 48 cm. Examination by light microscopy was carried out in a Vickers projection microscope; and for electron microscopy an EM 3 Metrovick apparatus and a Siemens Elmiskop I were used, at 75 and 80 kV. respectively, the detached portions of the dendritic deposits being supported on thin films of either 'formvar' or carbon condensed in vacuum.

3. Results

(a) Visual observations and optical microscopy

By direct observation it was found that the stage at which the polished cathode surface showed appreciable dimming of its reflectivity, i.e. roughening of the deposit surface, corresponded approximately to the time τ of deposition given by $i\sqrt{\tau} = $ constant, as found by Ibl & Trümpler (1952), whose data are represented by the curves drawn in Fig. 4. At a somewhat later stage the deposits developed a sooty black appearance, and some of the deposit, when scraped off and examined in the optical microscope, was seen to be in the form of small particles often of elongated and dendritic shapes. At still later stages, e.g. after a few minutes deposition, filaments of dendrites 1–2 mm. long had grown out into the solution normal to the cathode, though on switching off the current these filaments collapsed immediately; and on moving the cathode they readily became detached. No appreciable difference was observed in the results with polished stainless-steel substrates as compared with those using copper or silver substrates.

(b) Electron-diffraction results

Electron-diffraction patterns from the copper and silver substrates, polished as above, showed that the surface region consisted of randomly oriented crystals only a few tens of Å in mean diameter.

Fig. 4 shows the observed orientation of the copper deposited from $0.1M$ $CuSO_4$ solution at room temperature at various nominal current densities and deposition times. The full-line in Fig. 4 represents the stage of first visible roughening or dimming of an initially smooth polished copper cathode in deposition

from $0.1M$ $CuSO_4$, as observed by Ibl & Trümpler (1952), i.e. $i\sqrt{\tau} = 88.1$ mA. sec.$^{\frac{1}{2}}$ cm.$^{-2}$ which we also found to hold. It will be seen that we usually observed only weak-to-moderate preferred orientation, predominantly with a $\langle 110 \rangle$ lattice row normal to the cathode surface on the average, as in Fig. 1, though with wide spread from the mean. Fig. 2 illustrates the $\langle 210 \rangle$ orientation twice observed, in one specimen at 16 mA. cm.$^{-2}$ for 20 sec., and one at 100 mA. cm.$^{-2}$ for $\frac{1}{2}$ sec. The random crystal orientation of the thicker deposits at high current density seems likely to be largely due to the fragile, loose nature of these very dendritic deposits (cf. below in (c)). In all cases the electron-diffraction rings or arcs of Cu_2O were also present, the Cu_2O being usually in $\langle 110 \rangle$ orientation. No significant difference was observed between deposits on polished stainless steel and those on polished copper.

Copper deposits from $0.3M$ $CuSO_4$ solution, on polished copper, were also investigated at 100 mA.cm.$^{-2}$ current density and times of deposition of 4, 8 and 20 sec., but showed Cu in practically random orientation, though with some Cu_2O in a moderately developed $\langle 110 \rangle$ orientation on the 4-sec. deposit. For comparison it is noted that Ibl & Trümpler (1952) found for this solution: $i\sqrt{\tau} = 235$ mA.sec.$^{\frac{1}{2}}$ cm.$^{-2}$, thus at 100 mA.cm.$^{-2}$ $\tau = 5.8$ sec.

Our electron-diffraction observations on silver deposits on polished silver or stainless steel, from $0.1M$ $AgNO_3$, also showed only practically random crystal orientation in deposits at 20 mA.cm.$^{-2}$ for 4 sec., 40 mA.cm.$^{-2}$ for 1 sec., 60 mA.cm.$^{-2}$ for $\frac{1}{2}$ sec., and 100 mA.cm.$^{-2}$ for 2 sec.; but deposits at 40 mA.cm.$^{-2}$ for 2 sec. and 60 mA.cm.$^{-2}$ for 1 sec. yielded patterns closely similar to Fig. 2, indicating $\langle 210 \rangle$ orientation of the silver. For comparison Ibl & Trümpler (1952) found with this solution: $i\sqrt{\tau} = 62.9$ mA.sec.$^{\frac{1}{2}}$ cm.$^{-2}$, thus $\tau = 2.6$ sec. at 40 mA.cm.$^{-2}$, and 1.1 sec. at 60 mA.cm.$^{-2}$. Usually a moderately strong diffraction ring was observed slightly inside the face-centred cubic Ag 111 ring, in the position corresponding to the 100 ring of the alternative close-packed hexagonal structure. This clearly shows pronounced stacking faulting of the superposition of the {111} atom layers of the face-centred cubic structure.

The silver deposits on polished stainless steel substrates appeared in general to be closely similar in structure to those prepared on polished silver substrates.

(c) Observations by electron microscopy

Electron micrographs were recorded from detached portions of silver and copper deposits prepared from $0.1M$ $AgNO_3$ and 0.1 and $0.3M$ $CuSO_4$ solutions respectively.

The silver deposits examined were: at 100 mA.cm.$^{-2}$ for 4 sec. and 30 sec.: and 60 mA.cm.$^{-2}$ for 1 and 2 sec. The copper deposits examined were from $0.1M$ $CuSO_4$
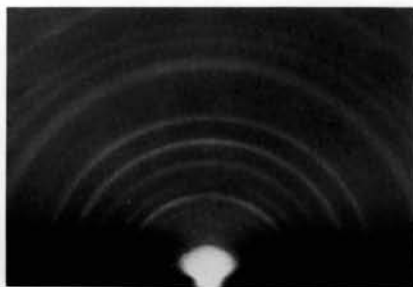
Fig. 1.
Cu from $0.1M$ $CuSO_4$ at 16 mA.cm.$^{-2}$ for
280 sec.; $\langle 110 \rangle$ orientation.
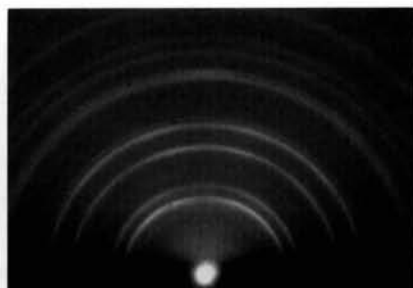

Fig. 2.
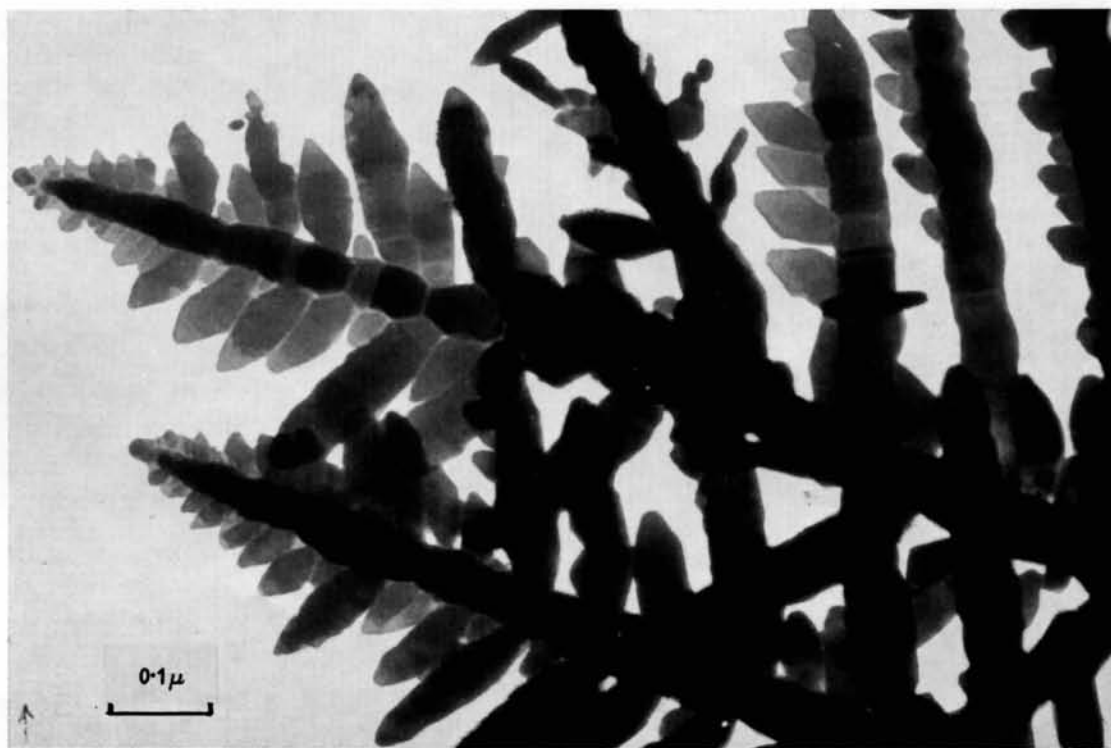As Fig. 1 but 20 sec.; $\langle 210 \rangle$ orientation.

Fig. 3(a).

Fig. 3(b).

Fig. 3. (a) Electron micrograph from Ag on Ag at 100 mA.cm.$^{-2}$ for 4 sec., from $0.1M$ $AgNO_3$.
(b) Enlargement of top left part of (a).

at 100 mA.cm.$^{-2}$ for 30 sec. and from 0·3M CuSO$_4$ for 20 sec.

All these silver and copper deposits yielded electron micrographs similar in type to Figs. 3(a) and (b), showing strongly dendritic structure. The following details of the dendrite form are observed:

(i) *The angle between the branches.*—Very frequently the branches of the dendrites were seen to be inclined at 60° or 120° to each other (cf. Fig. 3), and the stereomicrographs then showed that the plane common to these branches was practically normal to the axis of the microscope, and hence this angle was indeed the true angle between the branches. Departures from these angles were mostly found from examination of stereoscopic pairs of photographs to be due to a tilt of the plane of the two branches away from this orientation. In addition some branches or even main stems were clearly bent or otherwise damaged (cf. Fig. 3) during the preparation or handling of the specimen.

(ii) *The extent of the branching.*—The branching is repeated to several orders; for example Fig. 3(a) illustrates four orders of successive branching.

(iii) *The lengths of the branches.*—Near the outer tips which are roughly symmetrically surrounded by solution, the branches are approximately of equal length on each side of the stem, though in general not symmetrically in opposite pairs (cf. Fig. 3(b)). The mean locus of the tips of the side branches approximates to a straight line at about 30° to the central stem. This angle is presumably determined by the rate of forward growth of the stem in relation to the rate of diffusion of cations up to the cathode region. Further away from the region of the growing tips the side branches tend to have smaller secondary branches on them which are often only or mainly on the side facing towards the region of solution towards which the stem of the dendrite is growing (cf. Fig. 3(b)); this is less depleted of ions by their prior removal by attraction to the cathodic deposit than is the solution further back among the already formed dendrite side branches.

(iv) *The form of the branches near the outer tips of the dendrites.*—The branches at this early stage of formation are clearly mainly flat sheet-like crystals tending to be diamond- or rhomb-shaped with tip angle 60° (sometimes ∼ 50° where more rounded in form), but normally truncated by a straight short edge perpendicular to the long axis of the branch, with a corresponding parallel linear base where the branch joins the stem (cf. Fig. 3(b)). These flat crystal sheets often show signs of uneven thickness, and sometimes apparently growth steps; and often are thinned down towards the tip. Branches slightly further from the stem tips, and correspondingly thicker, often show re-entrant angles and cross lines indicating stepped or faceted form, with signs of incipient branching. As will be seen from Fig. 3(b) the rhomb-shaped branches near the tip of a dendrite tend to form a mosaic such

that the adjacent rhombs do not overlap but meet at a clearly defined junction line. This appears to confirm that the rhomb faces are all practically coplanar, at least on either side of the stem.

(v) *The form of the stems.*—A prominent feature of the stems, shown near the tips of the dendrites particularly clearly in Fig. 3(b), is that they are crossed at irregular intervals of the order of 300 Å by sharp light lines perpendicular to the stem axis. The reason for the lightness of these lines is not at present clear. They meet the sides of the stem at re-entrant angles, and the sides of these make an angle of 120° with the cross lines. The segments of stem between the cross lines are thus largely flat and bounded by edges at 120° to each other. Such faces, coplanar with the side-branch rhombs, must evidently be {111} planes bounded by ⟨110⟩ edges or (less likely) by ⟨211⟩ type of rows; thus the stems must be either ⟨211⟩ or ⟨110⟩ directions respectively. Further experiments are in progress to distinguish between these two possibilities. The most frequently observed ⟨110⟩ orientations of the deposit as a whole, indicated by the electron-diffraction reflection patterns, seems to suggest that the stems and branches are along ⟨110⟩ directions usually, as Layton also observed (1952).

The stem segments are not all of the same average thickness, and are sometimes not themselves uniform in thickness, differing by a factor of up to 2 or 3. The side branches grow out from the region where the cross lines meet the stem sides at the re-entrant angles, and in Fig. 3(b) there is seen to be a light line (similar to the cross lines) marking the junction of such branches with the stem. Not all the cross lines have a side branch associated with each of their ends.

4. Discussion

The present observations by electron microscopy show in detail the dendritic nature and form of the silver and copper deposits at a much earlier stage of growth than was studied by Finch & Layton (1951), but show similarly the strong tendency for the dendrites to be bounded by smooth {111} faces. They grow out along a densely-populated atom row which we conclude to be either a ⟨211⟩ or a ⟨110⟩ direction in such a face, with repeated branching at 60° along other such directions.

The process of development of the dendrites appears to be as follows. The rhomb-shaped lateral plate-like branches near the tip of a stem evidently grow in the usual manner, apparently by growth and spreading of layers of deposited atoms or ions on their surface, and largely tend to maintain the 60° rhomb form with the truncated tip, as the crystals grow larger. This growth thus involves the migration of deposited atoms or ions over the crystal surface.

The small rhomb at the extreme tip of a stem is of similar type, including the truncated tip, which is here normal to the stem axis. It is evident that when this

rhomb has grown to a certain size, some event—perhaps a stacking fault or dislocation such as is indeed indicated prominently by the hexagonal 100 ring in the diffraction pattern—occurs at the truncated end plane of the tip, causing nucleation of a new rhomb coplanar with the former leading one and with the same axis. This new rhomb grows (apparently faster than the previous end one) until its base coincides with the truncating end plane of the previous one, thereby corresponding to a cross-line of the stem like those in Fig. 3(b). It appears that as soon as this stage is reached, outgrowth of lateral branches, i.e. rhombs, commences. The existence of the white line separating the side of the stem from the lateral-branch crystals in Fig. 3(b) seems to support this view.

The deposit lattice orientation indicated most often by the reflection electron-diffraction patterns is of $\langle 110 \rangle$ type, which as above can arise from the observed $\{111\}$ habit of the crystal growth (Wilman, 1955). The $\langle 210 \rangle$ orientation observed in several cases must probably be associated with development of faces of some other form. We have, however, at present no detailed observations of the crystal habit in this case.
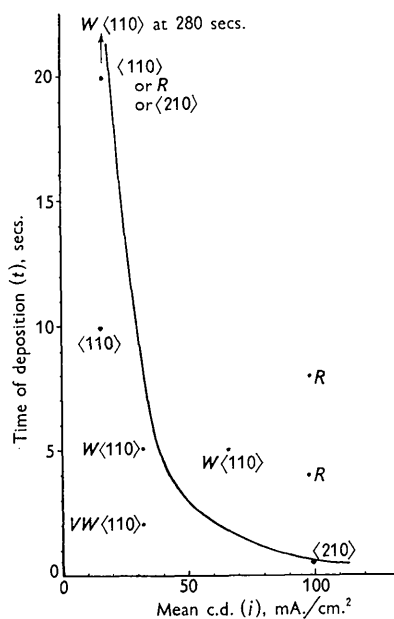
the dendrites. Previous theoretical considerations (cf. Ibl & Trümpler, 1952; Ibl, 1954) have indicated the relationship of this stage of growth to the fact that the supply of cations to the growing cathodic deposit is limited by the rate of diffusion of the ions from the solution further away. This favours preferential deposition of the cations on those parts of the deposit that project out most into the solution (cf. Finch, Wilman & Yang, 1947; Finch & Layton, 1951), and this in turn favours the development of a preferred crystal orientation. Those crystals eventually predominate that have the highest rate of growth normal to the cathode, i.e. presumably crystals having two or more main faces simultaneously normal to the cathode (Wilman, 1955).

A further correlation of the form of the deposit structure with the onset of the outward growth tendency, due to the limitation of the cation supply by their diffusion, is indicated by comparison of the results of Setty & Wilman (1955) with the relation $i\sqrt{\tau} = \text{constant}$, defining the stage of visible dimming. In the deposition of silver from a cyanide bath on to smooth $\{110\}$, $\{111\}$, and $\{100\}$ faces of a silver single crystal, Setty & Wilman observed that the mean deposit thickness at which the initial continuation of the substrate crystal lattice became accompanied by strong $\{111\}$ twinning decreased rapidly at first with increase in the current density, but then decreased less and less rapidly. A similar variation with current density was also observed for the deposit thickness

Fig. 4. Preferred mean orientation of Cu deposits on Cu from $0.1M$ CuSO$_4$, as a function of c.d. and time of deposition, determined by electron diffraction; $\langle 110 \rangle$ (or $\langle 210 \rangle$) denotes orientation with a $\langle 110 \rangle$ (or $\langle 210 \rangle$ respectively) row normal to the cathode; $R =$ random polycrystalline structure; $w =$ weak, $vw =$ very weak; the curve shows the locus of $i\sqrt{\tau} = 88.1$ mA.sec.$^{\frac{1}{2}}$.cm.$^{-2}$ for first visible dimming, as found by Ibl & Trümpler (1952).

The preferred orientation is seen (cf. Fig. 4) to be developed well before the stage of visible dimming of the cathode and to be usually of $\langle 110 \rangle$ type. It is clear that the stage of visible dimming of the cathode is a measure of the extent of the outward growth of
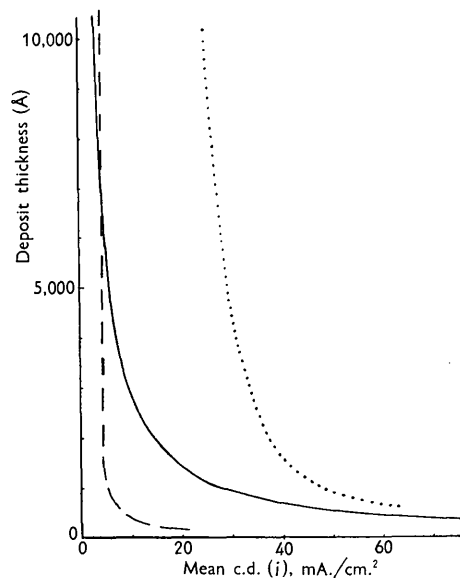

Fig. 5. The full line shows the variation of mean deposit thickness at the stage of first visible dimming, as a function of c.d., corresponding to Ibl & Trümpler's data for Cu (see Fig. 4). Also shown for comparison are the loci separating the continued single-crystal growth from the subsequent $\{111\}$-twinned growth (broken line at 20 °C., dotted locus at 40 °C.) found by Setty & Wilman (1955) for Ag on Ag (110) face, from a cyanide bath.

at which the twinned single-crystal structure gave place to random polycrystalline structure. That these stages of change of form of the deposit structure are closely related to the diffusion-controlled changes in the rate of supply of cations to the cathode (deposit) region, is clear if we convert the relation $i\sqrt{\tau} = $ constant to a relation between the current density (i) and the mean thickness D of the deposit, which was the variable used by Setty & Wilman. Thus, since the mean deposit thickness D_d at the stage of first visible dimming of the cathode, is proportional to $i\tau$, the above relation becomes:

$$iD_d = \text{constant.}$$

The plot of D_d against i is thus a rectangular hyperbola, similar in general form to the loci observed by Setty & Wilman, which delimit the region of thickness at which a change from one deposit-structure form to the next occurs (see Fig. 5).

We therefore conclude that the twin growth in this case was favoured when once initiated, and the twin orientations finally became strongly represented, because these orientations were favourable to more rapid outward growth and thus received more deposited ions by diffusion than crystals having other orientations. The fact that the stage of strong development of twinning was reached more quickly on the crystal substrate faces of type $\{110\}$ than $\{100\}$, and $\{100\}$ than $\{111\}$ must be attributed primarily to the relative tendencies for *initiation* of growth twins being in this order, which corresponds to an increasing number of available potential troughs in which atoms can be accommodated on these substrate surfaces, as Setty & Wilman pointed out. The rate of growth of the twins when these were once initiated must, however, have been affected also to some extent by the different orientation (possibly habit also) of the twins formed on these deposits on these substrate faces.

References

FINCH, G. I. & LAYTON, D. N. (1951). *J. Electrodepos. Tech. Soc.* **27**, 215.

FINCH, G. I. & SUN, C. H. (1936). *Trans. Faraday Soc.* **32**, 852.

FINCH, G. I. & WILLIAMS, A. L. (1937). *Trans. Faraday Soc.* **33**, 564.

FINCH, G. I. & WILMAN, H. (1937). *Ergebn. exakt. Naturw.* **16**, 353.

FINCH, G. I., WILMAN, H. & YANG, L. (1947). *Disc. Faraday Soc.* **1**, 144.

IBL, N. & TRÜMPLER, G. (1952). *Helv. Chim. Acta*, **35**, 363.

IBL, N. & TRÜMPLER, G. (1953). *Helv. Chim. Acta*, **36**, 2023.

IBL, N. (1954). *Helv. Chim. Acta*, **37**, 1149.

KANEKO, S. & KAWAMURA, K. (1940a). *Bl. Elektrochem. Lab.* **4**, 182.

KANEKO, S. & KAWAMURA, K. (1940b). *Chem. Abstr.* **36**, 4031_5.

KUDRA, O. K. (1934). *Mem. Inst. Chem. Acad. Sci. Ukrain. S.S.R.* **1**, 81.

KUDRA, O. K. (1935). *Mem. Inst. Chem. Acad. Sci. Ukrain. S.S.R.* **4**, 49, 385.

KUDRA, O. K. (1938a). *Mem. Inst. Chem. Acad. Sci. Ukrain. S.S.R.* **5**, 239.

KUDRA, O. K. (1938b). *Chem. Abstr.* **32**, 2435_9, 8277_9.

KUDRA, O. K. (1936). *Z. physikal. Chem.* A, **175**, 377.

LAYTON, D. N. (1952). *J. Electrodepos. Tech. Soc.* **28**, 239.

MODI, H. J. & TENDOLKAR, G. S. (1953). *J. Sci. Industrial Res. (India)*, **12**, No. 9.

SAND, H. J. S. (1900). *C. R. Acad. Sci., Paris*, **131** (II), 992.

SANDS, H. J. S. (1901). *Phil. Mag.* **1**, 45.

SEBBORN, W. S. (1933). *Trans. Faraday Soc.* **29**, 825.

SETTY, T. H. V. & WILMAN, H. (1955). *Trans. Faraday Soc.* **51**, 984.

ULLMAN, C. (1897). *Z. Elektrochem.* **3**, 516.

WILMAN, H. (1955). *Trans. Inst. Metal Finishing*, **32**, 281.

WRANGLEN, G. (1950). *Z. Electrochem. Soc.* **97**, 353.